Journal of Molecular Catalysis B: Enzymatic 75 (2012) 11–19

Contents lists available at SciVerse ScienceDirect

Journal of Molecular Catalysis B: Enzymatic

journal homepage: www.elsevier.com/locate/molcatb

Unravelling the suicide inactivation of tyrosinase: A discrimination between mechanisms

Jose Luis Muñoz-Muñoz[a], Jose Berna[b], Francisco Garcia-Molina[a], Pedro Antonio Garcia-Ruiz[c], Jose Tudela[a], Jose N. Rodriguez-Lopez[a], Francisco Garcia-Canovas[a,*]

[a] *GENZ: Grupo de Investigación Enzimología, Departamento de Bioquímica y Biología Molecular-A, Facultad de Biología, Universidad de Murcia, E-30100 Espinardo, Murcia, Spain*
[b] *Departamento de Química Orgánica, Facultad de Química, Universidad de Murcia, E-30100 Espinardo, Murcia, Spain*
[c] *QCPAI: Grupo de Química de Carbohidratos, Polímeros y Aditivos Industriales, Departamento de Química Orgánica, Facultad de Química, Universidad de Murcia, E-3010 Espinardo, Murcia, Spain*

ARTICLE INFO

Article history:
Received 5 May 2011
Received in revised form 5 October 2011
Accepted 1 November 2011
Available online 15 November 2011

Keywords:
Tyrosinase
Suicide inactivation
3,6-Difluorocatechol
3-Isopropyl-6-methylcatechol
3-*tert*-Butyl-6-methylcatechol
Irreversible inhibition

ABSTRACT

The suicide inactivation kinetics of tyrosinase acting on 3-isopropyl-6-methylcatechol, 3-*tert*-butyl-6-methylcatechol and 3,6-difluorocatechol was studied. All three substrates act as suicide substrates despite the fact that their 3 and 6 positions are occupied, confirming the mechanism proposed in Biochem. J. (2008) 416, 431–440. Although the most active substrate for the suicide inactivation was 3,6-difluorocatechol, its efficiency was much lower than that of the catechol used as reference. Its *r* value, the number of turnovers made by one mol of enzyme before its inactivation, is the highest described in the bibliography, highlighting the great difference between the catalytic and inactivation constants. A study of the effect of the pH on the enzymatic activity of tyrosinase showed that both 3-isopropyl-6-methylcatechol and 3-*tert*-butyl-6-methylcatechol behave as typical substrates of tyrosinase, while 3,6-difluorocatechol behaves differently. The remarkable behavior of 3,6-difluorocatechol when reacts with tyrosinase may be due to the fact that its two hydroxyl groups have very low p*K* values as a result of the strong electron-withdrawing effect of the fluorine atoms in the *ortho* positions, so that, at pH 7.0, the substrate would be mainly negatively charged. The apparent Michaelis constant shows a minimum value at pH 6.0, but increases at both high and low pH. However, the values of the catalytic constant and maximum apparent inactivation constant do not vary with the pH, so that the *r* remains practically constant. Under anaerobic conditions, 3,6-difluorocatechol acts as an irreversible inhibitor of the deoxy- and met-tyrosinase forms.

1. Introduction

Tyrosinase is a cuproprotein that catalyses the hydroxylation of monophenols to *o*-diphenols and the oxidation of the latter to *o*-quinones [1–5]. It has long been known that the enzyme is inactivated when it acts on *o*-diphenols [6–12]. This property of tyrosinase has been studied from several perspectives and the most relevant aspects can be summarized as follows: (i) the process does not occur by means of free radicals; (ii) it does not occur through an attack on the part of the *o*-quinone generated or any aminoacid from the active centre; (iii) during the process half of the copper content of the enzyme is released [13,14].

As indicated above, the *o*-diphenols inactivate the enzyme but only alter many catalytic cycles, in agreement with parameter, "*r*" (the number of turnovers made by one mol of enzyme before being inactivated). However, the *o*-diphenols in only one catalytic cycle manage to convert the met-tyrosinase form, which is inactive towards monophenols, to deoxy-tyrosinase, which, with O_2, is converted to *oxy*-tyrosinase, a form that acts on the monophenols [3,15,16].

The kinetics of the suicide inactivation of tyrosinase was studied some time ago [8], while a more systematic study on the kinetics of the steady-state and transition phase was carried out later [17–21]. The progress made in the study of the tyrosinase structure [22–26] has enabled greater insight into the underlying mechanisms of the suicide inactivation of tyrosinase [1,14,27–37].

Two models, which share certain aspects and diverge considerably in others (Schemes 1 and 2) have been proposed to explain the suicide inactivation of tyrosinase in its action on *o*-diphenolic substrates [14,33]. In both cases, it is suggested that one of the copper atoms at the active centre is reduced to Cu^0 and is released, thus inactivating the enzyme [13]. Other authors [33], suggest that the enzyme hydroxylates the *o*-diphenols because it considers them as another form of monophenol. According to this model, a compound

* Corresponding author. Tel.: +34 868 884764; fax: +34 868 883963.
E-mail address: canovasf@um.es (F. Garcia-Canovas).

1381-1177/$ – see front matter © 2011 Elsevier B.V. All rights reserved.
doi:10.1016/j.molcatb.2011.11.001

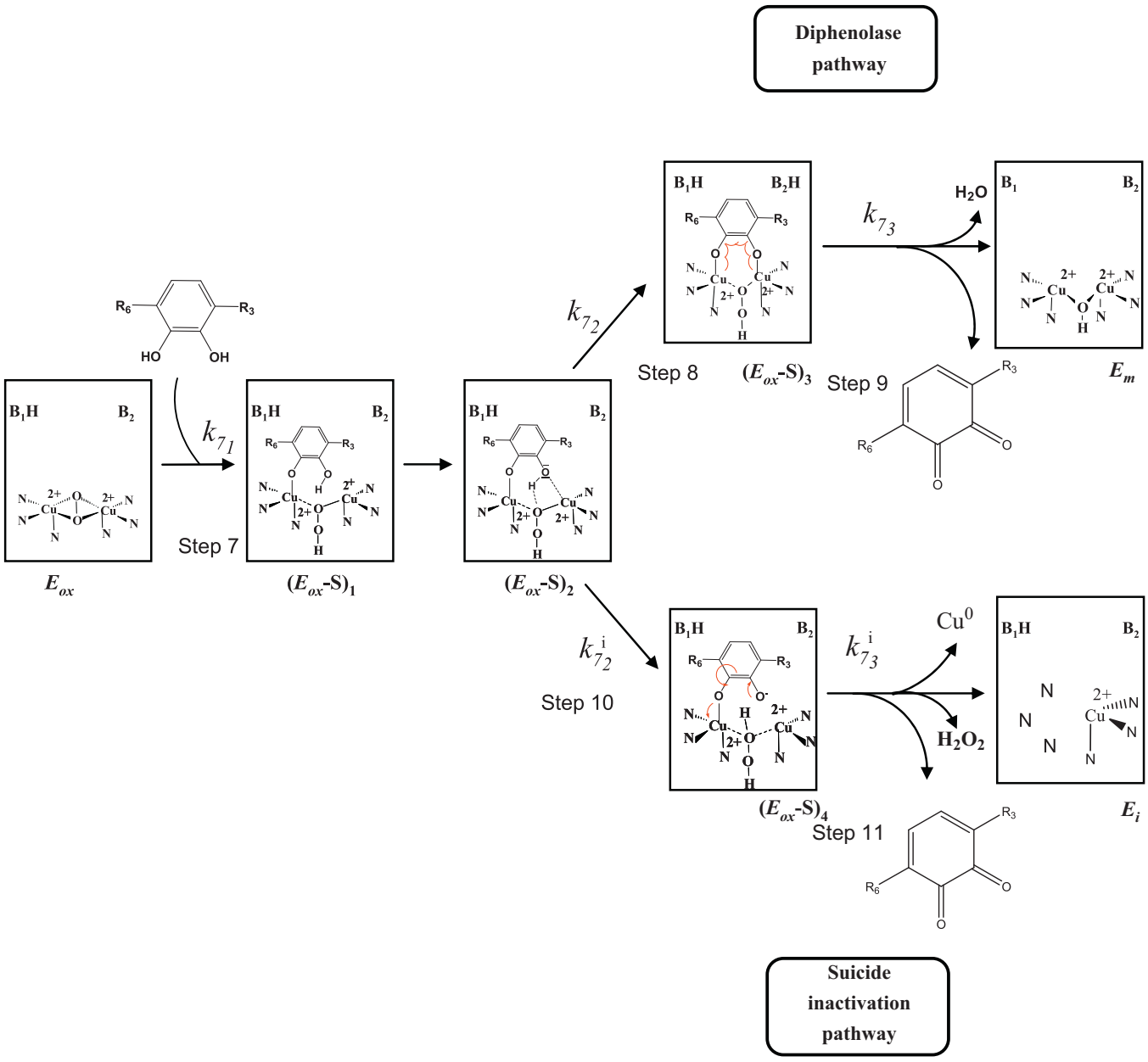

Scheme 1. Kinetic mechanism proposed to explain the diphenolase and suicide inactivation pathways of tyrosinase action on *o*-diphenols. E_{ox}, *oxy*-tyrosinase; $(E_{ox}\text{-S})_1$, *oxy*-tyrosinase/substrate complex axially bound to a Cu atom and with the proton of hydroxyl group transferred to the peroxide group; $(E_{ox}\text{-S})_2$, *oxy*-tyrosinase/substrate complex forming a hydrogen bond; $(E_{ox}\text{-S})_3$, *oxy*-tyrosinase/substrate complex axially bound to the two Cu atoms; $(E_{ox}\text{-S})_4$, *oxy*-tyrosinase/substrate complex axially bound to one Cu atom and the deprotonated hydroxyl group of C-2; E_m, *met*-tyrosinase; E_i, enzyme inactive.

like pyrogallol (1,2,3-trihydroxybenzene) would not lead to suicide inactivation of the enzyme. In a previous work, our group showed that all *o*-diphenols and triphenols are suicide substrates of tyrosinase, the most potent being pyrogallol [14]. The mechanism proposed in Scheme 1 covers the possibility of suicide inactivation during the oxidation of *o*-diphenols and triphenols like gallic acid or pyrogallol since it is the way in which one proton of substrate is transferred to the active centre of the enzyme which triggers its suicide inactivation mechanism. The mechanism of Scheme 1 predicts that the suicide inactivation of the enzyme would occur regardless of what R_3, R_4 and R_6 are. However, according to the mechanism proposed in Scheme 2, if the substituents in 3 and 6 positions are different from hydrogen, that is R_3 and $R_6 \neq H$, suicide inactivation would not occur.

In a subsequent series of studies, different authors [33–37] claim to have experimentally demonstrated the validity of the mechanism proposed in Scheme 2. For our part, we have demonstrated that compounds like ascorbic acid [38], tetrahydropterines [39], NADH [40] and tetrahydrofolic acid [41] behave as suicide substrates. According to our mechanism (Scheme 1), any of the substrates of tyrosinase studied – *o*-diphenols, triphenols, ascorbic acid or such different molecules as NADH, tetrahydropterines or tetrahydrofolic acid – may inactivate the enzyme, since this process would occur as long as there was the possibility of a proton being transferred from the substrate to a base B_2 (perhaps glutamic acid [26] or a histidine not bound to the copper) or to the peroxide group. Note that this possibility would exist in all substrates of tyrosinase in which suicide inactivation has been described [14,38–41].

In an attempt to differentiate the two mechanisms, Quintox' Group [35,36] synthesized 3,6-difluorocatechol, a compound which, according to the model proposed by these authors (Scheme 2), should not induce suicide inactivation because the 3

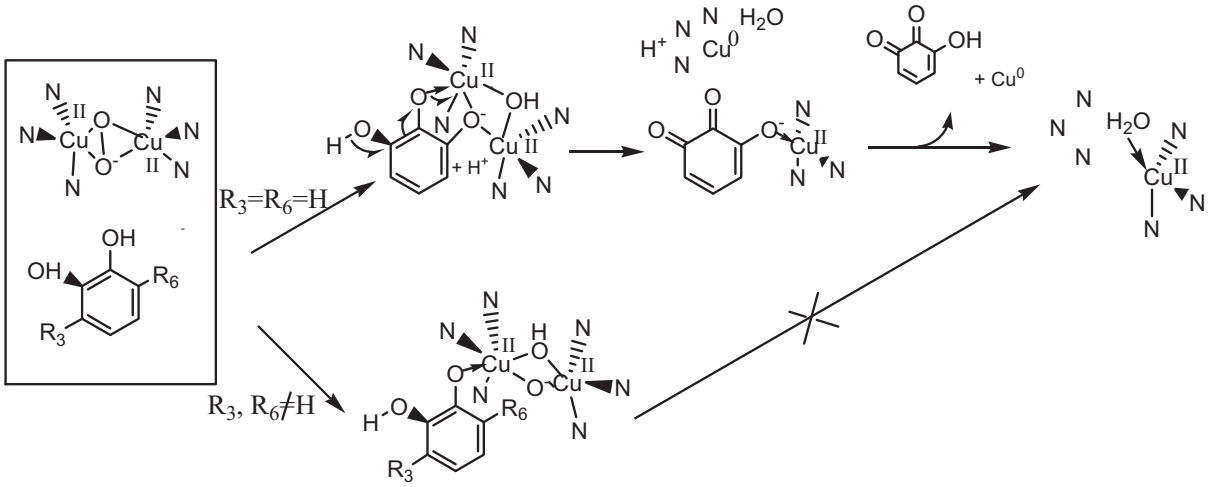

Scheme 2. Proposed model to explain the suicide inactivation of tyrosinase during its monophenolase activity when it acts on *o*-diphenols [33].

and 6 positions are occupied by fluorine atoms, and then it cannot be hydroxylated by the enzyme.

With the aim to discriminate between the proposed models, our group has studied the inactivation kinetics of tyrosinase by the catechol-derived compounds with their 3 and 6 positions substituted, in this case 3-isopropyl-6-methylcatechol (3I6MCat) and 3-*tert*-butyl-6-methylcatechol (3T6MCat). Furthermore, we synthesized 3,6-difluorocatechol (3,6DFCat). The results show that all three 3,6-disubstituted substrates studied behave as suicide substrates of tyrosinase, confirming Scheme 1.

2. Experimental

2.1. Materials

Mushroom tyrosinase or polyphenol oxidase (TYR, *o*-diphenol: O_2 oxidoreductase, EC 1.14.18.1) (8300 units/mg) and β-NADH were supplied by Sigma (Madrid, Spain). The enzyme was purified as previously described in [42]. Protein concentration was determined by the Lowry method [43]. The substrates used 3-isopropyl-6-methylcatechol (3I6MCat) and 3-*tert*-butyl-6-methylcatechol (3T6MCat) (Fig. 1) were purchased from Sigma (Madrid, Spain). All other chemicals were of analytical grade. Stock solutions of the diphenolic substrates were prepared in 0.15 mM phosphoric acid to prevent autooxidation. Milli-Q system (Millipore corp.) ultrapure water was used throughout.

2.2. Methods

2.2.1. Preparation of 3,6-difluorocatechol (3,6DFCat)

3,6-Difluorocatechol (3,6DFCat, Fig. 1) was synthesized from the commercially available 1,2,3,4-tetrafluorobenzene (CAS: 551-62-2) following the three-step methodology reported by Ladd et al. [44].

2.2.2. Characterization of 3,6-difluorocatechol (3,6DFCat)

^{1}H- and ^{13}C NMR spectra were recorded at 298 K on a Bruker Avance 400 MHz instrument. ^{1}H NMR chemical shifts are reported relative to Me_4Si and were referenced via residual proton resonances of the corresponding deuterated solvent whereas ^{13}C NMR spectra are reported relative to Me_4Si using the carbon signals of the deuterated solvent. Detailed physical data for 3,6DFCat are listed in the supplementary material and are complementary to those reported in the literature [44].

2.2.3. Dialysis

To know whether TYR was irreversibly inactivated by 3,6DFCat, the residual enzyme activity of TYR/3,6DFCat mixtures was measured before and after dialysis. The effect of dialysis on TYR/3,6DFCat mixture was tested as follows: TYR (2 nM) in 30 mM sodium phosphate buffer (pH 6.0) was preincubated with 12 mM of 3,6DFCat (in the case of the suicide inactivation reaction, aerobic conditions) and 0.5 mM of 3,6DFCat (in the case of E_d inhibition, anaerobic conditions) for 2 h, in both cases at room temperature. Each sample was placed into the dialysis membrane (Sigma, Madrid, Spain) with a molecular weight cut-off of 6000–8000 Da and then dialyzed overnight against two changes of 30 mM sodium phosphate buffer (pH 6.0) to remove the 3,6DFCat. Enzyme activity before and after dialysis was measured in a spectrophotometer by adding 100 μL of the dialyzed solution to the cuvette containing 900 μL of 9 mM TBC, 30 mM sodium phosphate buffer (pH 6.0) and 0.2 mM NADH.

2.2.4. Spectrophotometric assays

These assays were carried out with a Perkin-Elmer Lambda-35 (Perkin-Elmer, Massachusetts, USA) spectrophotometer, on line interfaced to a PC-computer, where the kinetic data were recorded, stored and later analyzed. The product of the enzyme reaction *o*-quinone is unstable and evolves towards melanins [45]. For this reason, the reaction was followed by measuring the disappearance

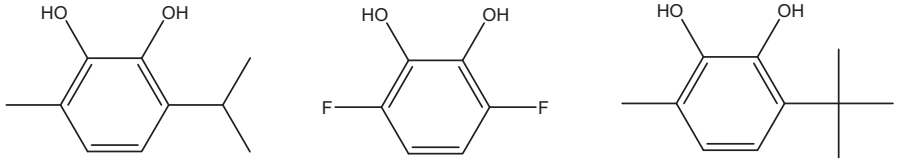

Fig. 1. Chemical structures of the substrates used in this work.

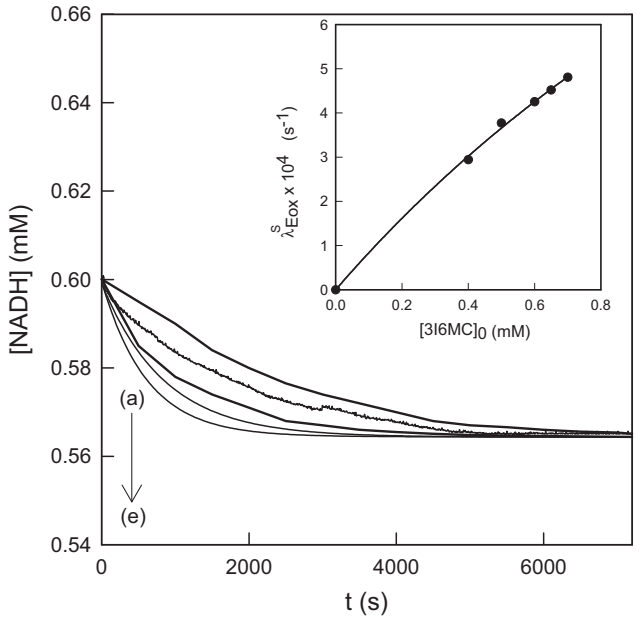

Fig. 2. Corrected recordings of the disappearance of NADH in the suicide inactivation of tyrosinase by different 3-isopropyl-6-methylcatechol concentrations. The experimental conditions were 30 mM sodium phosphate buffer (pH 7.0), 0.26 mM O_2, wavelength = 380 nm, and the initial concentrations of NADH and tyrosinase were 0.6 mM and 2.2 nM, respectively. The substrate concentrations were (mM): (a) 4, (b) 5, (c) 6, (d) 6.5 and (e) 7. Inset. Values of $\lambda^S_{E_{ox}}$ for different 3-isopropyl-6-methylcatechol concentrations.

of NADH at 340 nm, with $\varepsilon = 6230\,M^{-1}\,cm^{-1}$, which reduces *o*-quinone to *o*-diphenol or measuring the AH_2 disappearance at 262 nm, with $\varepsilon = 11{,}100\,M^{-1}\,cm^{-1}$ [46].

2.2.5. Kinetic data analysis

The experimental data of time-based assays for the disappearance of NADH (Fig. 2) follow Eq. (1):

$$[NADH] = [NADH]_f + [NADH]_\infty e^{-\lambda^S_{Eox} t} \quad (1)$$

where $[NADH]_f$ is the NADH-value at $t \to \infty$, $[NADH]_\infty = [Q]_\infty$ is the NADH consumed at the end of the reaction and $\lambda^S_{E_{ox}}$ is the apparent constant of suicide inactivation of tyrosinase in the presence of *o*-diphenol. These parameters can be obtained by non-linear regression [47]. There is always a slow spontaneous oxidation of *o*-diphenol and NADH (result not shown), which should be computer corrected in further NADH *vs*. time plots (in general this treatment is applied to all the kinetic recordings).

2.2.6. Generation of E_{ox} and E^R_d

We set out to kinetically characterize the inactivation of E^R_d (relaxed form of deoxy-tyrosinase). For this, E^R_d was generated from the native enzyme, adding micromolar concentrations (5 μM) of H_2O_2 so that the E_m form passed to E_{ox}. Then nitrogen was bubbled through the solution transforming all the E_{ox} to E^R_d ($E_{ox} \rightleftarrows E^R_d + O_2$) [42,48,49]. This enzyme sample was used to study the reaction of E^R_d with 3,6DFCat.

2.2.7. Generation of E^T_d

To generate the enzyme form E^T_d (tense form of deoxy-tyrosinase), E^R_d was allowed to evolve to E^T_d under anaerobic conditions for 90 min [42,48,49].

2.2.8. Generation of E_m

The inactivation of E_m was characterized by first generating it from the native enzyme in two ways: (a) adding 2 μM catalase, so that $E_{ox} \rightleftarrows E_m + H_2O_2$; catalase acts on the H_2O_2 displacing the equilibrium, $2H_2O_2 + \text{catalase} \rightarrow O_2 + 2H_2O$, so that E_{ox} is transformed into E_m. (b) Adding 5 μM of H_2O_2, so that all the enzyme passes to E_{ox} and then adding 2 μM catalase [48,49]. This enzyme sample was used to study the reaction of E_m with 3,6DFCat.

3. Results and discussion

In order to distinguish the mechanisms proposed to explain the suicide inactivation of tyrosinase (Schemes 1 and 2), three *o*-diphenolic substrates (derivatives of catechol) were studied, all with positions 3 and 6 occupied: 3-isopropyl-6-methylcatechol (3I6MCat), 3-*tert*-butyl-6-methylcatechol (3T6MCat) and 3,6-difluorocatechol (3,6DFCat) (Fig. 1).

3.1. Kinetic characterization of 3I6MCat as suicide substrate of tyrosinase

Fig. 2 shows the experimental recordings of the suicide inactivation of tyrosinase acting on 3I6MCat at pH 7.0, where the disappearance of NADH as coupled reagent is shown as it reduces the *o*-quinone to *o*-diphenol. The two-stage experimental design studied variations in substrate and enzyme concentrations.

3.1.1. Effect of substrate concentration

Fig. 2 shows the effect of varying the substrate concentration (at pH 7.0) while keeping the enzyme concentration constant. Non-linear regression analysis of these records in accordance with Eq. (1) gives the values of $\lambda^S_{E_{ox}}$ and $[NADH]_\infty$. Fig. 2 inset shows the variation of $\lambda^S_{E_{ox}}$ with regard to substrate concentration. The lineal behavior reflects the fact that the enzyme cannot be saturated by the substrate due to its molecular size. In agreement with Eq. (2), the slope of the straight line gives the value of the inactivation efficiency ($\lambda^S_{E_{ox}(max)}/K^S_m$), whose value is shown in Table 1 [14]:

$$\lambda^S_{E_{ox}} = \frac{\lambda^S_{E_{ox}\,(max)}[S]_0}{K^S_m + [S]_0} \quad (2)$$

3.1.2. Varying the enzyme concentration

The recordings of the suicide inactivation of tyrosinase acting on 3I6MCat at pH 7.0 are shown in Fig. 1SM, keeping the substrate concentration constant and varying the initial concentration of enzyme. Non-linear regression analysis of these records in accordance with Eq. (1) gives the values of $\lambda^S_{E_{ox}}$ and $[NADH]_\infty$. The Inset shows how the values of $\lambda^S_{E_{ox}}$ and $[NADH]_\infty$ vary with respect to the initial enzyme concentration. As can be seen, the apparent inactivation constant is independent of enzyme concentration (●). The slope of the straight line has a value of 2*r*, as determined from the linear dependence of $[NADH]_\infty$ on $[E]_0$ (○) (Fig. 1SM inset). The values of *r*, the number of turnovers made by one mol of enzyme before its inactivation, and of $\lambda^S_{E_{ox}(max)}/K^S_m$, the inactivation efficiency, are shown in Table 1.

3.2. Kinetic characterization of 3T6MCat as suicide substrate of tyrosinase

Following the same procedure as in the case of 3I6MCat, the inactivation efficiency ($\lambda^S_{E_{ox}(max)}/K^S_m$) and *r*, the partition ratio or the turnover numbers made by one mol of enzyme before its inactivation, can be obtained (see Figs. 2SM and 3SM and Table 1). Considering the data from Table 1, while the *r* values are of the same order of magnitude, the inactivation efficiency of 3I6MCat

Table 1
Kinetic constants characterizing the suicide inactivation of tyrosinase acting on 3,6-disubstituted *o*-diphenols.

	pH	$\lambda^S_{E_{ox}(max)} \times 10^4$ (s^{-1})	r[b]	k^S_{cat} (s^{-1})	K^S_m (mM)	k^S_{cat}/K^S_m ($s^{-1}\,M^{-1}$)	$\lambda^S_{E_{ox}(max)}/K^S_m \times 10^2$ ($s^{-1}\,M^{-1}$)	δ_1 (ppm.)	δ_2 (ppm)
3,6DFCat	4.0	5.55 ± 0.29	190156 ± 8211	105 ± 14	2.57 ± 0.29	(40 ± 5) × 10^3	21.6 ± 2.4		
	5.0	5.76 ± 0.35	194840 ± 8050	112 ± 13	2.19 ± 0.27	(51 ± 6) × 10^3	26.3 ± 3.5		
	5.5	5.83 ± 0.21	190010 ± 8888	110 ± 11	1.42 ± 0.15	(77 ± 9) × 10^3	41.1 ± 4.6		
	6.0	5.92 ± 0.25	182222 ± 7996	107 ± 10	0.77 ± 0.08	(139 ± 16) × 10^3	76.9 ± 8.3		
	7.0	5.81 ± 0.29	198744 ± 8902	115 ± 11	1.66 ± 0.18	(69 ± 8) × 10^3	35.0 ± 3.9	133.48	133.48
	8.0	5.99 ± 0.31	188848 ± 8137	113 ± 14	2.93 ± 0.33	(38 ± 4) × 10^3	20.4 ± 2.1		
3I6MCat	7.0	–	6890 ± 214	–	–	(38 ± 2) × 10^1	6 ± 0.5	146.70	144.00
3T6MCat	7.0	–	1613 ± 73	–	–	148 ± 6	7.7 ± 0.4	146.60	142.90
Cat[a]	7.0	89.20 ± 2.70	99994 ± 1604	874 ± 30	0.16 ± 0.01	(5463 ± 589) × 10^3	5575.0 ± 61.8	146.59	146.59

[a] Data taken from Ref. [14].
[b] Obtained from transition phase kinetic studies.

is one order of magnitude greater than that of 3T6MCat. Dialysis experiments, as described in Section 2, showed that the inactivated enzyme had no activity.

3.3. Kinetic characterization of 3,6DFCat as suicide substrate of tyrosinase

When the kinetic experiments were carried out with 3,6DFCat at pH 7.0, apparently no inactivation of tyrosinase was observed, at least on the time scale depicted in Fig. 4SM. However, inactivation was more apparent when the pH was lowered (Fig. 4SM). Table 1 shows the carbon-13 NMR chemical shifts (δ values) of the investigated substrates. It is noteworthy the low δ values of the carbons that support the hydroxyl groups of 3,6DFCat which is indicative the low p*K* values (≅7.2) of these groups. At pH 7.0, more than half of this fluorinated catechol is deprotonated and, consequently, the substrate is negatively charged which might explain the results obtained, as we shall see later. Note the wide difference from the δ values of the other compounds (Table 1), indicating that at pH 7.0 the hydroxyl groups of the other substrates are completely protonated.

3.4. Some considerations on the kinetic parameters of 3I6MCat and 3T6MCat

As mentioned above, the size and low solubility of these substrates mean that the enzyme cannot be saturated. From the experimental data obtained (Fig. 2 and Figs. 1SM–4SM), it is only possible to obtain the parameter "*r*" (the number of turnovers that one mol of enzyme makes before being inactivated) and the inactivation efficiency, $\lambda^S_{E_{ox}(max)}/K^S_m$. Note that the substrates have practically the same steric hindrance since the isopropyl group behaves like the *tert*-butyl group, which is equivalent to saying that the K^S_m should be practically the same, so that the maximum apparent inactivation constant, ($\lambda^S_{E_{ox}(max)}$) for 3T6MCat may be one order of magnitude higher than that for 3I6MCat (see Table 1).

The value of r ($k^S_{cat}/\lambda^S_{E_{ox}(max)}$) is greater for 3I6MCat than for 3T6MCat, which is in agreement with the higher value of $\lambda^S_{E_{ox}(max)}$ predicted for 3T6MCat (Table 1). However, although the catalytic constant for 3T6MCat should be greater than for 3I6MCat according to the values of δ_1 and δ_2 (Table 1), this increase is less than the increase in $\lambda^S_{E_{ox}(max)}$.

From measurements of the steady-state, V_0 can be obtained for each of the substrates, while a graph of $V_0/[E]_0$ *vs.* $[S]_0$, provides the catalytic efficiency (k^S_{cat}/K^S_m) (Fig. 5SM). The relation between k^S_{cat}/K^S_m and the inactivation efficiency $\lambda^S_{E_{ox}(max)}/K^S_m$ (Fig. 5SM inset) provides the value of r (Table 1). Therefore, a study of the transition phase and the steady-state with respect to initial substrate concentration provides r-values (6333 ± 621 for 3I6MCat and 1922 ± 203 for 3T6MCat), which practically coincide with those obtained from the analysis of the transition phase data with respect to variations in the initial enzyme concentration (Figs. 1SM and 3SM and Table 1).

3.5. Effect of pH on the oxidation of 3,6DFCat, 3I6MCat and 3T6MCat by tyrosinase

From the measurements of the initial velocity at different pH values, the dependence of V_0 *vs.* pH can be obtained. Fig. 3 shows these values – it can be seen that both 3I6MCat and 3T6MCat behave as typical tyrosinase substrates, with a sigmoidal dependence of V_0 *vs.* pH (indicating the existence of an apparent kinetically significant p*K*), while 3,6DFCat shows a bell shape, suggesting the existence of two apparents significant p*K*s. A sigmoidal curve is typical when the effect of pH on the kinetic of the oxidation of *o*-diphenols is studied, as can be seen in the case of catechol (Cat) (Fig. 3 inset A). This curve is of the same type although the substrates have charges in their R group of carbon 4 [48,50].

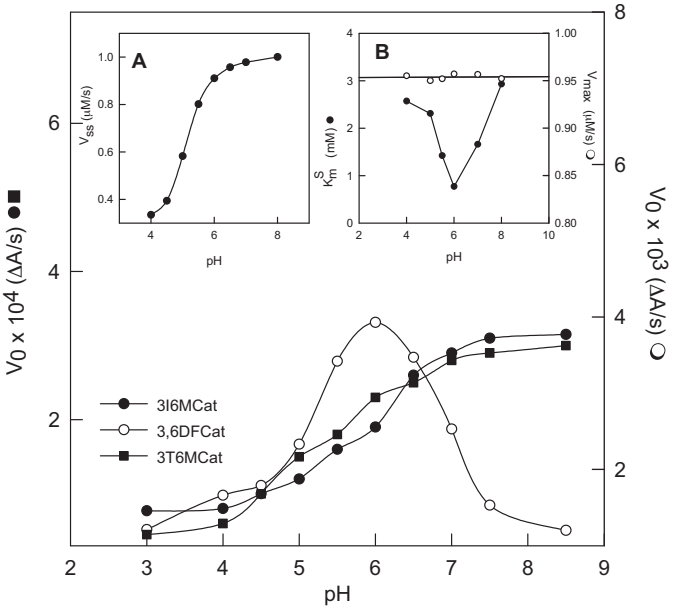

Fig. 3. Representation of the values of V_0 *vs.* pH for every substrates, (○) 3,6DFCat, (●) 3I6MCat and (■) 3T6MCat. The experimental conditions were 30 mM sodium acetate buffer (pH 3.0–5.5) or 30 mM sodium phosphate buffer (pH 6.0–8.5), 0.15 mM NADH, 0.26 mM O_2, wavelength = 340 nm (3T6MCat and 3,6DFCat) and 380 nm (3I6MCat), $[3,6DFCat]_0$ = 12 mM, $[3I6MCat]_0$ = 5 mM, $[3T6MCat]_0$ = 0.5 mM and $[E]_0$ = 0.05 nM for 3,6DFCat and 0.1 nM for 3I6MCat and 3T6MCat. Inset A. Representation of the ascorbic acid disappearance rates in the oxidation of Cat by tyrosinase rate at wavelength = 262 nm (V^{262}_{ss}) *vs.* pH, $[AH_2]_0$ = 50 μM, $[Cat]_0$ = 0.2 mM and $[E]_0$ = 1 nM. Inset B. Representation of K^S_m (●) and V^S_{max} (○) *vs.* pH for 3,6DFCat.

$$(E_d^R)^{2-} + 2H^+ \rightleftharpoons (E_d^R)^{-+} + 2H^+ \rightleftharpoons (E_d^R)^{2+}$$

$$(E_{ox})^{2-} + 2H^+ \rightleftharpoons (E_{ox})^{-+} + 2H^+ \rightleftharpoons (E_{ox})^{2+}$$

$$(E_m)^{2-} + 2H^+ \rightleftharpoons (E_m)^{-+} + 2H^+ \rightleftharpoons (E_m)^{2+}$$

Scheme 3. Kinetic mechanism to explain the effect of pH on the different enzymatic forms of tyrosinase in its catalytic cycle.

The substrate 3,6DFCat may have two negative charges at high pH, which may explain its behavior with respect to the steady-state data shown in Fig. 3 (○) and to the suicide inactivation seen in the experimental registers of Fig. 4SM. The existence of two apparents critical p*K* in the enzyme was revealed in a previous work on deoxytyrosinase based on a study of the transition of the deoxy form (relaxed) to another form (tense) with the copper atoms more separated [49]. Scheme 3 reflects the existence of two apparents p*K* in each of the enzymatic forms that exist in the catalytic cycle of tyrosinase.

An *o*-diphenolic substrate of tyrosinase with no charge, as is the case of Cat, provides V_0 *vs.* pH curve as seen in Fig. 3 inset A, with an apparent kinetically significant p*K*. This behavior can be explained if the form $(E)^{2+}$ is not active on the substrate since for its binding it would be necessary form a hydrogen bond with the hydroxyl group, accept a proton and therefore generate a nucleophilic reagent (like O^-) to attack the copper. The proton may be captured by the forms $(E)^{2-}$ and $(E)^{+-}$ and so the apparent p*K* involved in the step $(E)^{2-} + 2H^+ \rightleftarrows (E)^{-+}$ will not be kinetically significant; therefore, apparently only one significant p*K* exists since the form $(E)^{2+}$ is inactive. However, since the p*K* of the hydroxyl groups is low, the substrate 3,6DFCat may have two negative charges at pH 7.0 and thus demonstrate the two apparent p*K*s of the enzymatic forms (Scheme 3). Thus, at high pH values, the enzyme is in the form $(E)^{2-}$ and the substrate in the form $(S)^{2-}$; consequently, the enzyme will show low affinity for the substrate, the initial velocity will decrease substantially and the suicide inactivation will be very slow (very low apparent inactivation constant $\lambda^S_{E_{ox}}$). As the pH of the medium falls, enzyme activity will increase (greater affinity for the substrate) and the process of suicide inactivation now becomes evident (higher $\lambda^S_{E_{ox}}$, Fig. 4SM). Therefore, at low pH values, the suicide inactivation by 3,6DFCat can be studied (time scale of around 6000 s), the enzyme is in the form $(E)^{+-}$ and the substrate $(S)^0$. As the pH fallen further, the enzyme will be in the form $(E)^{2+}$ and the substrate $(S)^0$, so that the enzymatic activity falls (Fig. 3) and the suicide inactivation apparently becomes slower (Fig. 4SM).

3.6. Effect of pH on the steady-state parameters, V_{max} and K^S_m

We studied the effect of pH on the enzymatic activity and determined the values of the kinetic parameters at each pH value assayed. The non-dependence of V_{max} (○) *vs.* pH and the parabolic dependence of K^S_m (●) are evident in Fig. 3 inset B. The behavior of V_{max} is typical of tyrosinase substrates since this parameter depends on the nucleophilic power of the oxygens of the phenolic hydroxyls. However, the value of K^S_m shows a parabolic dependence, indicating that the enzyme shows maximum affinity for the substrate when it occurs as $(E)^{+-}$ and the substrate with protonated hydroxyl groups as $(S)^0$.

3.7. Kinetic characterization of 3,6DFCat as suicide substrate of tyrosinase

3.7.1. Effect of substrate concentration

The experimental registers of the suicide inactivation of tyrosinase acting on 3,6DFCat are shown in Fig. 4A (at pH 5.0). The

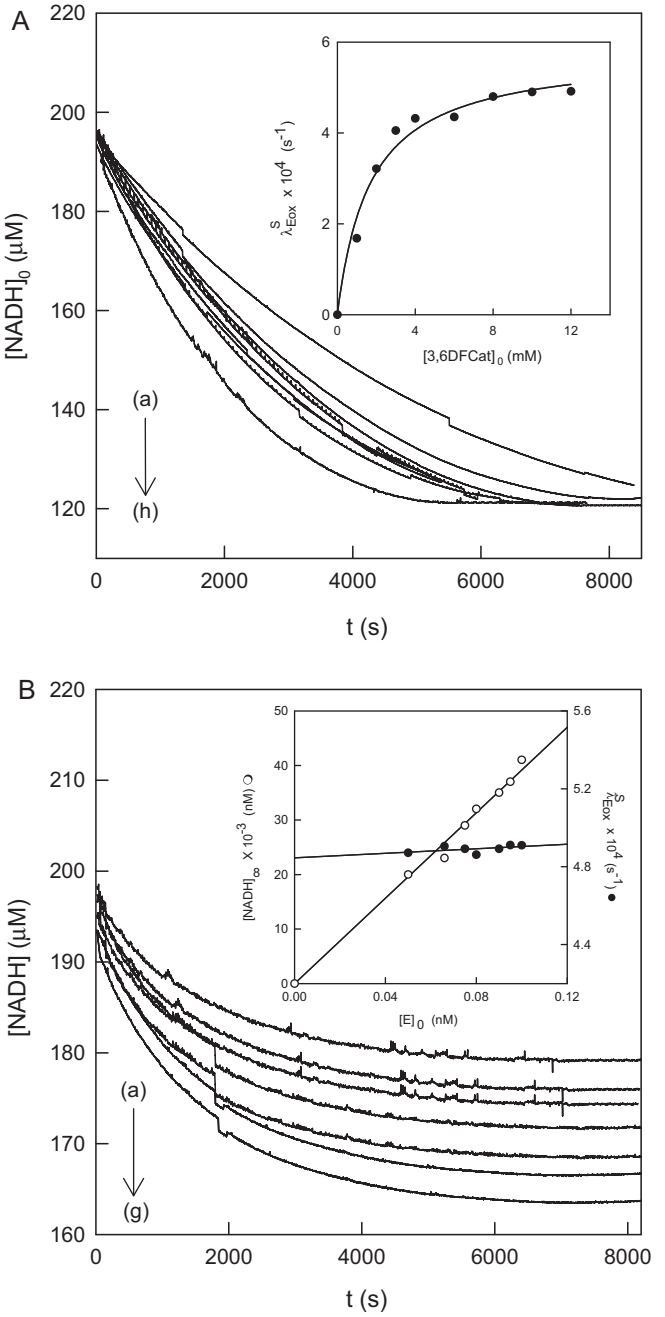

Fig. 4. (A) Corrected recordings of the disappearance of NADH in the suicide inactivation of tyrosinase by different 3,6DFCat concentrations. The experimental conditions were 30 mM sodium phosphate buffer (pH 5.0), 0.26 mM O_2, wavelength = 340 nm and the initial concentrations of NADH and tyrosinase were: 0.2 mM and 0.2 nM, respectively. The substrate concentrations were (mM): (a) 1, (b) 2, (c) 3, (d) 4, (e) 6, (f) 8, (g) 10 and (h) 12. Inset. Values of $\lambda^S_{E_{ox}}$ for different 3,6DFCat concentrations. (B) Corrected recordings of the disappearance of NADH in the suicide inactivation of tyrosinase by 3,6DFCat for different enzyme concentrations. The experimental conditions were 30 mM sodium phosphate buffer (pH 5.0), 0.2 mM NADH, 0.26 mM O_2, wavelength = 340 nm, $[3,6DFCat]_0$ = 12 mM and $[E]_0$ (nM): (a) 0.05, (b) 0.06, (c) 0.075, (d) 0.08, (e) 0.09, (f) 0.095 and (g) 0.1. Inset. Representation of the values of $[NADH]_\infty$ (○) and $\lambda^S_{E_{ox}}$ (●) *vs.* enzyme concentration.

non-linear regression analysis of these registers in accordance with Eq. (1) provides the parameters $\lambda^S_{E_{ox}}$ and $[NADH]_\infty$ [14]. In this case, as can be seen from Fig. 4A inset, the enzyme is saturated and $\lambda^S_{E_{ox}(max)}$ and K^S_m can be calculated (see Table 1). The inactivation efficiency $\lambda^S_{E_{ox}(max)}/K^S_m$, which is shown in Table 1, is higher than those obtained with the other two 3,6-disubstituted

catechols studied, but much lower than the catechol used as reference (Table 1).

3.7.2. Effect of enzyme concentration

Fig. 4B shows the effect of enzyme concentration when working at a constant substrate concentration at pH 5.0. Fig. 4B inset depicts the values obtained for $[NADH]_\infty$ *vs.* $[E]_0$. The slope has a value of 2*r*, giving a value of $r = k^S_{cat}/\lambda^S_{E_{ox}(max)} = 194,840 \pm 8050$. Note that this *r* is the highest described in the literature, meaning that the lower the value of the chemical shift of δ in C-1 and C-2 (see Table 1), the greater the nucleophilic power of the hydroxyl group's oxygen. This will facilitate the attack of the oxygen on the copper centre of tyrosinase and, subsequently, the transfer of the proton of the hydroxyl group to the base B_2 or the transfer of the proton of the hydroxyl group to the oxygen of the peroxide group, thus provoking inactivation. So, the kinetic and inactivation constants will be more separated and so the value of *r* will be higher.

3.8. Effect of pH on the kinetic of the suicide inactivation of tyrosinase by 3,6DFCat

As mentioned above, in a study of the effect of pH on the steady-state parameters, the apparent Michaelis constant is lowest at pH 6.0, and, in agreement with Eq. (2), the apparent inactivation constant will vary with the pH. A study of the effect of pH on the kinetics of suicide inactivation pointed to a hyperbolic dependence on substrate concentration (Fig. 4A inset). At both high and low pH values, $\lambda^S_{E_{ox}}$ decreases because K^S_m increases, and registers must be made on a greater time scale. However, the results obtained from fitting $\lambda^S_{E_{ox}}$ *vs.* $[S]_0$ provides the values of K^S_m and $\lambda^S_{E_{ox}(max)}$. Table 1 shows these values, which reflect the fact that the two processes of catalysis (k^S_{cat}) and inactivation ($\lambda^S_{E_{ox}(max)}$) are pH-independent, which means that the "*r*" is also pH-independent (Table 1). It should be noted that 3,6DFCat has the highest *r* described in the literature (maximum difference between k^S_{cat} and $\lambda^S_{E_{ox}(max)}$), although the catalytic (k^S_{cat}/K^S_m) and inactivation ($\lambda^S_{E_{ox}(max)}/K^S_m$) efficiencies, while higher than for 3I6MCat and 3T6MCat, are much lower than for catechol (Cat, Table 1).

In Table 1 it is possible to compare 3,6DFCat with catechol at pH 7.0. As can be seen, the K^S_m for 3,6DFCat is higher, although the catalytic efficiency is lower despite the lower values of δ. This may be due to the presence of fluorine groups in 3 and 6 positions, which would hamper the binding of the substrate to the enzyme and so lead to a lower k^S_{cat} and higher K^S_m. Note how the k^S_{cat} and the *r* values of 3,6DFCat do not agree with the results obtained for *o*-diphenols with hydrogen atoms at the 3 and 6 positions [14].

Therefore 3,6DFCat behaves as a suicide substrate according to the mechanism depicted in Scheme 1, and in turn confirms the reliability of this model. According to recent publications [3,51–53], the mechanism proposed to explain the suicide inactivation of tyrosinase takes into account the existence of two p*K*s for the enzyme acting on 3,6-DFCat (Fig. 3). The complete mechanism is depicted in Supplementary material. Scheme 1 shows the most important steps in the inactivation. One molecule of substrate 3,6DFCat interacts with the form E_{ox} of the enzyme. Since base B_1 is protonated, the oxygen of the hydroxyl group bound to the carbon atom with the lowest value of δ, can carry out a nucleophilic attack on the copper atom (*CuB*) and transfer the proton of the same hydroxyl group to the peroxide group of the form E_{ox}, this being the slowest catalytic step. Subsequently, the oxygen atom of the second hydroxyl group bound to the carbon atom with the highest δ carries out the nucleophilic attack on the other copper atom (*CuA*) and base B_2 accepts the proton. Another possibility is that the proton of the second hydroxyl group is transferred to the peroxide group that is already protonated, in which case the suicide inactivation of the enzyme will occur in what would be the slowest step of the process (see Tables 1 and 2).

Table 2
Kinetic constants characterizing the inactivation of E^R_d, E_m and E^T_d by 3,6DFCat under anaerobic conditions.

Enzymatic form	K_S (mM)	k_{i_S} (min^{-1})	k_{i_S}/K_S ($min^{-1}\,mM^{-1}$)
E^T_d	0.14 ± 0.02	0.093 ± 0.008	0.66 ± 0.09
E^R_d	0.11 ± 0.02	0.345 ± 0.034	3.13 ± 0.49
E_m	0.11 ± 0.02	0.345 ± 0.034	3.13 ± 0.49

Above, it has demonstrated that under aerobic conditions, 3,6DFCat acts as a suicide substrate of tyrosinase, while below we disclose the study of the irreversible inhibition of tyrosinase by the same substrate, but under anaerobic conditions.

3.9. Inactivation of tyrosinase by 3,6DFCat under anaerobic conditions

Under anaerobic conditions, the enzyme is irreversibly inactivated in the presence of 3,6DFCat. The enzymatic forms present under anaerobic conditions are: deoxy-tyrosinase (E_d) and met-tyrosinase (E_m). Furthermore, the form E_d undergoes a transition in such conditions to another form, as described in [49]. By analogy with hemocyanin [54], these forms are denominated E^R_d (relaxed) and E^T_d (tense). Fig. 6SM depicts the transition of E^R_d to E^T_d and, again by analogy with hemocyanin [54], the copper atoms are considered to be more separated in E^T_d (Scheme ISM). Note that the forms E_m and E_{ox} do not undergo transition (Fig. 6SM), probably because the binding between the copper atoms in these forms precludes their separation. In the case of E_m it is a hydroxyl group and in E_{ox} a peroxide group (Scheme ISM) [2,49].

The enzymatic form E^R_d is inactivated by 3,6DFCat with a first order kinetics that depends on the pH (Fig. 5). Data analysis according to:

$$[E^R_d]_t = [E^R_d]_0 e^{-\lambda^S_{E^R_d} t} \quad (3)$$

gives the value of $\lambda^S_{E^R_d}$. The apparent inactivation constant varies with the pH (Fig. 5 inset), data which are in agreement with those of Fig. 3 inset B. The apparent inactivation constant is maximum at pH 6.0, at which value the Michaelis constant is minimal.

Fig. 7SM depicts the variation of 3,6DFCat concentration, at optimal pH. Analysis according to Eq. (3) gives the values of $\lambda^S_{E^R_d}$. The values of this constant ($\lambda^S_{E^R_d}$) is represented *vs.* the initial concentration of 3,6DFCat and the analysis of Eq. (4) enables us to obtain the values of $k^R_{i_S}$ and K^R_S (Table 2):

$$\lambda^S_{E^R_d} = \frac{k^R_{i_S}[S]_0}{K^R_S + [S]_0} \quad (4)$$

When E^R_d is allowed to evolve for 90 min under anaerobic conditions, it is converted into the form E^T_d (Scheme ISM). A similar study of the inactivation of E^T_d (Figs. 8SM and 9SM) provides the data contained in Table 2. When the inactivation of the form E_m is studied, its transformation into E^R_d first occurs and then is inactivated according to Scheme 4 (Table 2).

The forms E^R_d and E_m show greater substrate affinity and higher inactivation constants. This may be due to the greater distance between the copper atoms at the active centre of the E^T_d form of tyrosinase, as occurs with hemocyanin [54]. Both in experiments carried out under aerobic conditions (suicide inactivation) and under anaerobic conditions (that lead to irreversible inactivation), dialysis of the samples and the determination of enzymatic activity reveal that the enzyme is irreversibly inactivated.

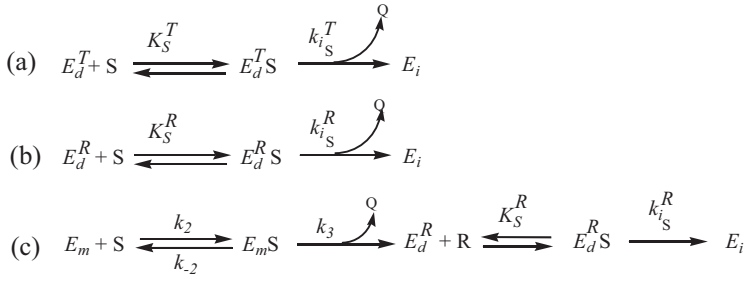

Scheme 4. Kinetic mechanism showing the inhibition of E_d^T, E_d^R and E_m by 3,6DFCat.

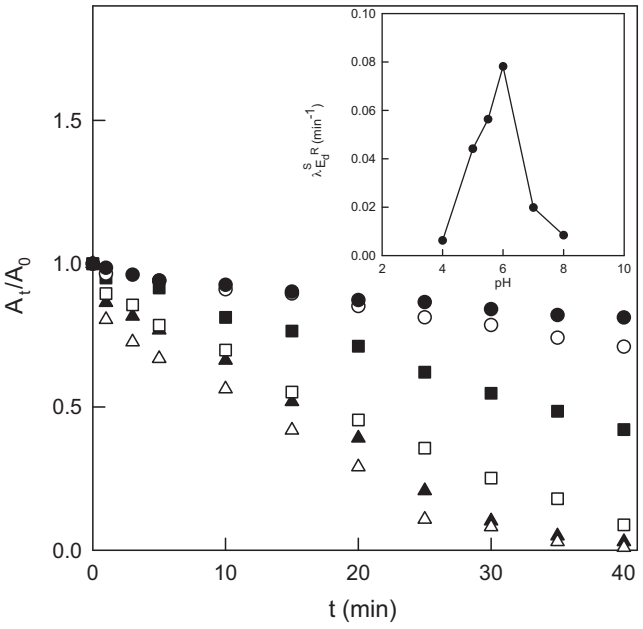

Fig. 5. Inactivation of the E_d^R form of TYR by 3,6DFCat at different pH. The form E_d^R was generated (see Section 2) and immediately incubated with 3,6DFCat, taking aliquots at different times to measure the residual activity with 9 mM TBC (wavelength = 410 nm). The values obtained were fitted to Eq. (3), and the apparent inactivation constant ($\lambda^S_{E_d^R}$) was obtained at each pH. The experimental conditions were: 30 mM sodium acetate buffer (pH 4.0–5.5) or 30 mM sodium phosphate buffer (pH 6.0–8.0) at 25 °C, $[E]_0$ 0.2 μM (see Section 2), $[H_2O_2]_0$ 5 μM [3,6DFCat]$_0$ = 50 μM and the pH-values used were: 4.0 (●), 8.0 (○), 7.0 (■), 5.0 (□), 5.5 (▲) and 6.0 (△). Inset. Representation of $\lambda^S_{E_d^R}$ *vs.* pH.

4. Conclusions

The compounds derived from catechol, 3,6-disubstituted, behave as suicide substrates of tyrosinase under aerobic conditions, confirming the validity of the mechanism proposed in Scheme 1. 3,6-Difluorocatechol shows a different kinetic behavior from all the *o*-diphenols studied for this enzyme [14]: (i) the K_m^S *vs.* pH follows a parabolic behavior, (ii) its action mechanism points to the existence of two critical apparent p*K*s in the enzyme, (iii) the *r*-value is the highest described in the literature, which explains the great difference between the catalytic and inactivation constants. Under anaerobic conditions, 3,6-difluorocatechol irreversibly inactivates the enzyme.

Acknowledgements

This paper was partially supported by grants from the Ministerio de Educación y Ciencia (Madrid, Spain) Project BIO2009-12956, from the Fundación Séneca (CARM, Murcia, Spain) Projects 08856/PI/08 and 08595/PI/08 and from the Consejería de Educación (CARM, Murcia, Spain) BIO-BMC 06/01-0004. FGM and JLMM have fellowships from Fundación Caja Murcia (Murcia, Spain). J.B. thanks the MICINN for a Ramón y Cajal Fellowship, cofinanced by the European Social Fund.

Appendix A. Supplementary data

Supplementary data associated with this article can be found, in the online version, at doi:10.1016/j.molcatb.2011.11.001.

References

[1] J.L. Muñoz-Muñoz, F. Garcia-Molina, R. Varon, P.A. Garcia-Ruiz, J. Tudela, F. Garcia-Canovas, J.N. Rodriguez-Lopez, IUBMB Life 62 (2010) 539–547.
[2] E.I. Solomon, U.M. Sundaram, T.E. Machonkin, Chem. Rev. 96 (1996) 2563–2606.
[3] M. Rolff, J. Schottenheim, H. Decker, F. Tuczek, Chem. Soc. Rev. 40 (2011) 4077–4098.
[4] S.M. Marino, S. Fogal, M. Bisaglia, S. Moro, G. Scartabelli, L. De Gioia, A. Spada, E. Monzani, L. Casella, S. Mammi, L. Bubacco, Arch. Biochem. Biophys. 505 (2011) 67–74.
[5] G. Battaini, E. Monzani, L. Casella, L. Lonardi, A.W. Tepper, G.W. Canters, L. Bubacco, J. Biol. Chem. 277 (2002) 44606–44612.
[6] J.M. Nelson, C.R. Dawson, Adv. Enzymol. 4 (1944) 99–152.
[7] I. Asimov, C.R. Dawson, J. Am. Chem. Soc. 72 (1950) 820–828.
[8] L.L. Ingraham, J. Corse, B. Makower, J. Am. Chem. Soc. 74 (1952) 2623–2626.
[9] Y. Tomita, M. Seiji, J. Dermatol. 4 (1977) 245–249.
[10] M. Seiji, M. Sasaki, Y. Tomita, Tohoku J. Exp. Med. 125 (1978) 233–245.
[11] Y. Tomita, A. Hariu, C. Mizuno, M. Seiji, J. Invest. Dermatol. 75 (1980) 379–382.
[12] K. Lerch, Mol. Cell. Biochem. 52 (1983) 125–138.
[13] C. Dietler, K. Lerch, in: T.E. King, H.S. Mason, M. Morrison (Eds.), Oxidases and Related Redox Systems, Pergamon Press, New York, 1982, pp. 305–317.
[14] J.L. Muñoz-Muñoz, F. Garcia-Molina, P.A. Garcia-Ruiz, M. Molina-Alarcon, J. Tudela, F. Garcia-Canovas, J.N. Rodriguez-Lopez, Biochem. J. 416 (2008) 431–440.
[15] A. Sanchez-Ferrer, J.N. Rodriguez-Lopez, F. Garcia-Canovas, F. Garcia-Carmona, Biochim. Biophys. Acta 1247 (1995) 1–11.
[16] J.R. Ros, J.N. Rodriguez-Lopez, F. Garcia-Canovas, Biochim. Biophys. Acta 1204 (1994) 33–42.
[17] F. Garcia-Canovas, J. Tudela, C. Martinez-Madrid, R. Varon, F. Garcia-Carmona, J.A. Lozano, Biochim. Biophys. Acta 912 (1987) 417–423.
[18] J. Tudela, F. Garcia Canovas, R. Varon, F. Garcia Carmona, J. Galvez, J.A. Lozano, Biochim. Biophys. Acta 912 (1987) 408–416.
[19] J. Escribano, J. Tudela, F. Garcia-Carmona, F. Garcia-Canovas, Biochem. J. 262 (1989) 597–603.
[20] S.G. Waley, Biochem. J. 185 (1980) 771–773.
[21] S.G. Waley, Biochem. J. 227 (1985) 843–849.
[22] Y. Matoba, T. Kumagai, A. Yamamoto, H. Yoshitsu, M. Sugiyama, J. Biol. Chem. 281 (2006) 8981–8990.
[23] M. Sendovski, M. Kanteev, V. Shuster Ben-Yosef, N. Adir, A. Fishman, Acta Crystallogr. Sect. F, Struct. Biol. Cryst. Commun. 66 (2010) 1101–1103.
[24] M. Sendovski, M. Kanteev, V. Shuster Ben-Yosef, N. Adir, A. Fishman, J. Mol. Biol. 405 (2011) 227–237.
[25] W.T. Ismaya, H.J. Rozeboom, A. Weijn, J.J. Mes, F. Fusetti, H.J. Wichers, W.B. Dijkstra, Biochemistry 50 (2011) 5477–5486.
[26] Y. Li, Y. Wang, H. Jiang, J. Deng, Proc. Natl. Acad. Sci. U.S.A. 106 (2009) 17002–17006.
[27] S. Chazarra, J. Cabanes, J. Escribano, F. Garcia-Carmona, Biochim. Biophys. Acta 1339 (1997) 297–303.
[28] T.S. Chang, J. Agric. Food Chem. 55 (2007) 2010–2015.
[29] T.S. Chang, Int. J. Mol. Sci. 16 (2009) 2440–2475.
[30] T.S. Chang, M.Y. Lin, H.J. Lin, J. Cosmet. Sci. 61 (2010) 205–210.
[31] S.S.-K. Tai, C.-G. Lin, M.-H. Wu, T.S. Chang, Int. J. Mol. Sci. 10 (2009) 4257–4266.

[32] J.L. Muñoz-Muñoz, J.R. Acosta-Motos, F. Garcia-Molina, R. Varon, P.A. Garcia-Ruíz, J. Tudela, F. Garcia-Cánovas, J.N. Rodríguez-López, Biochim. Biophys. Acta 1804 (2010) 1467–1475.
[33] E.J. Land, C.A. Ramsden, P.A. Riley, Tohoku J. Exp. Med. 212 (2007) 341–348.
[34] E.J. Land, C.A. Ramsden, P.A. Riley, M.R. Stratford, Tohoku J. Exp. Med. 216 (2008) 231–238.
[35] C.A. Ramsden, M.R.L. Stratford, P.A. Riley, Org. Biomol. Chem. 7 (2009) 3388–3390.
[36] C.A. Ramsden, P.A. Riley, ARKIVOC (i) (2010) 260–274.
[37] C.A. Ramsden, P.A. Riley, ARKIVOC (x) (2010) 248–254.
[38] J.L. Munoz-Munoz, F. Garcia-Molina, P.A. Garcia-Ruiz, R. Varon, J. Tudela, F. Garcia-Canovas, J.N. Rodriguez-Lopez, Biochim. Biophys. Acta 1794 (2009) 244–253.
[39] J.L. Munoz-Munoz, F. Garcia-Molina, E. Arribas, P.A. Garcia-Ruiz, J. Tudela, F. Garcia-Canovas, J.N. Rodriguez-Lopez, J. Enzyme Inhib. Med. Chem. 26 (2011) 728–733.
[40] F. Garcia-Molina, J.L. Munoz-Munoz, M. Garcia-Molina, P.A. Garcia-Ruiz, J. Tudela, F. Garcia-Canovas, J.N. Rodriguez-Lopez, Biosci. Biotechnol. Biochem. 74 (2010) 1777–1787.
[41] F. Garcia-Molina, J.L. Munoz-Munoz, F. Martinez-Ortiz, P.A. Garcia-Ruiz, J. Tudela, F. Garcia-Canovas, J.N. Rodriguez-Lopez, J. Agric. Food Chem. 59 (2011) 1383–1391.
[42] J.N. Rodriguez-Lopez, L.G. Fenoll, P.A. Garcia-Ruiz, R. Varon, J. Tudela, R.N. Thorneley, F. Garcia-Canovas, Biochemistry 39 (2000) 10497–10506.
[43] O.H. Lowry, N.J. Rosebrough, A.L. Farr, R.J. Randall, J. Biol. Chem. 19 (1951) 265–275.
[44] D.L. Ladd, J. Weinstock, J. Org. Chem. 46 (1981) 203–206.
[45] F. Garcia-Carmona, F. Garcia-Canovas, J.L. Iborra, J.A. Lozano, Biochim. Biophys. Acta 717 (1982) 124–131.
[46] F. Garcia-Molina, J.L. Muñoz, R. Varon, J.N. Rodriguez-Lopez, F. Garcia-Canovas, J. Tudela, J. Agric. Food Chem. 55 (2007) 9739–9749.
[47] Jandel scientific, Sigma Plot 9.0 for Windows™, Jandel scientific, Core Madera, 2006.
[48] F. Garcia-Molina, A.N. Hiner, L.G. Fenoll, J.N. Rodriguez-Lopez, F. Garcia-Canovas, J. Tudela, J. Agric. Food Chem. 53 (2005) 3702–3709.
[49] J.L. Munoz-Munoz, F. Garcia-Molina, P.A. Garcia-Ruiz, R. Varon, J. Tudela, F. Garcia-Canovas, J.N. Rodríguez-Lopez, J. Mol. Catal. B: Enzymatic 62 (2010) 173–182.
[50] M. Garcia-Moreno, R. Varon, A. Sanchez Gracia, J. Tudela, F. Garcia Canovas, Biochim. Biophys. Acta 1205 (1994) 282–288.
[51] I. Koval, P. Gamez, C. Belle, K. Selmeczi, J. Reedijk, Chem. Soc. Rev. 35 (2006) 814–840.
[52] A.W.J.W. Tepper, L. Bubacco, G.W. Canters, J. Biol. Chem. 277 (2002) 30436–30444.
[53] A.W.J.W. Tepper, L. Bubacco, G.W. Canters, J. Biol. Chem. 279 (2004) 13425–13434.
[54] M. Metz, E.I. Solomon, J. Am. Chem. Soc. 123 (2001) 4938–4950.